Mechanics of Advanced Composite Structures 11 (2024) 191 – 202

Semnan University

Mechanics of Advanced Composite Structures

journal homepage: http://MACS.journals.semnan.ac.ir

Comparison of Deflection in Two-Directional Functionally Graded Tapered Beam

G. C. M. Reddy [a*], P. Bridjesh [a], B. S. Reddy [b], K. V. K. Reddy [c]

[a] *Department of Mechanical Engineering, MLR Institute of Technology, Hyderabad, India*
[b] *Department of Mechanical Engineering, Rajeev Gandhi Memorial College of Engineering &Technology, Nandyal, India.*
[c] *Department of Mechanical Engineering, JNTU Hyderabad, Hyderabad, India.*

KEYWORDS

Comparison of deflection;

Reddy's higher order shear Deformation theory;

Two-Dimensional functionally graded taper beam;

Hamilton's principle;

Static responses.

ABSTRACT

Traditional engineering materials lack the necessary properties that are needed in aerospace as well as other modern industries. In order to address the aforementioned problem, a number of different materials are used in concert. With the help of functionally graded material, all the necessary characteristics can be achieved. A fast transition between two different materials can lead to debonding, thermal stresses, residual stresses, and stress concentrations; a gradual change in material properties might mitigate these problems. This work provides a comparison of the analytical solutions for the deflections in Two Dimensional Functionally Graded Taper Beam (2D-FGTB) under a uniformly distributed load, adapting Reddy's higher-order shear deformation theory. All the material properties of the beam are graded along the thickness and length dimensions using the power-law formula. The thickness of the beam is assumed to change linearly along its length. Equations of motion are derived based on Hamilton's principle and Navier's solutions. A parametric investigation is conducted to explore the effects of various material and geometrical parameters on the mechanics of 2D-FGTB. These parameters are found to be very significant in studying the static responses of 2D-FGTB.

1. Introduction

Functionally Graded Material (FGM) [1] was developed in Japan in the mid-1980s for structural and functional applications requiring high-temperature resistance and strength. FGM is an advanced composite material with dimension-dependent properties. High-temperature FGMs are inhomogeneous composites made of ceramic and metal phases. FGM effortlessly changes mechanical and physical properties by mixing metal and ceramic at suitable volumes. Ceramic resists high temperatures due to low thermal conductivity [2]. Ductile metal can withstand high-temperature gradient stresses for a short time [3]. Thus, low and high-temperature FGM structural components can use metals and ceramics. FGM is mostly used in structural applications that integrate refractoriness and toughness. Rocket engine combustion chambers, high-performance tools, etc. Heat shields in spacecraft, tubes in a heat exchanger, implants in biomedical applications, and fusion reactor plasma facings can use FGMs [4, 5]. Chemical facilities, nuclear reactors, aircraft, and other incompatible applications use FGM [6]. High-temperature thermal barrier coatings attach ceramic layers to metallic structures.

In high-temperature applications, a beam's end surfaces often have different temperatures (top and bottom). Consequently, the member is subjected to thermal loading because steady-state conditions facilitate heat conduction across the beam thickness [7].

Beam theories describe beam-type structures. Euler–Bernoulli beam theory is the oldest and most famous beam theory is Classical Beam Theory (CBT). Top and bottom shear stress violates free boundary conditions. First-order

* Corresponding author. Tel.: +91-77738403
E-mail address: cmreddy115@gmail.com

DOI: 10.22075/macs.2023.29871.1478
Received 2023-02-14; Received in revised form 2023-06-09; Accepted 2023-07-07.

shear deformation theory's shear force discrepancy requires a shear correction factor (k) [8]. Researchers developed Higher Order Shear Deformation Theory (HSDT) to overcome this problem. Shear deformation is widely noticeable in the thick beam. Beam theory ignores these effects. HSDT must accurately describe thick beam bending behavior, including cross-sectional warping. Appropriate kinematics and constitutive models enable this. The higher-order theory is accounted for transverse shear deformation by incorporating the function f(x) into the displacement field [9-10].

Ebrahimi et al. [11] using a Navier-type solution, this work investigates the free vibration characteristics of Functionally Graded (FG) nanobeams based on the third-order shear deformation beam theory. Material properties of FG nanobeam should vary continuously along the thickness according to the power-law model. The nonlocal governing equations are developed using Hamilton's principle and third-order shear deformation beam theory, then solved using an analytic solution. Cukanovi et al. [12] describe the bending analysis of thick and moderately thick FG square and rectangular plates on a Winkler-Pasternak elastic basis. The plates are assumed to have an isotropic, two-component material distribution throughout their thickness, with the modulus of elasticity increasing in terms of the volume percentages of the constituents according to a power-law distribution. Sayyad [13] the purpose of their work was to create a unified theory of shear deformation based on displacements to study advanced composite beams and plates that are susceptible to shear deformation. In order to model transverse shear deformation, a variety of coordinate shape functions based on trigonometry, hyperbola, parabola, and exponential were created. Bending and shear rotations affected in-plane displacements. This theory's parabolic shape function produces Reddy's theory. Prashik Malhari Ramteke et al. [14] in this study, the nonlinear Eigen frequency responses of an FGM panel in a temperature environment are computed using finite elements. Consideration is given to the elements of the FGM as a function of temperature. The material properties of the FGM panel are evaluated using Voigt's micromechanical model in conjunction with three unique material distribution patterns. Thom et al. [15] Two-Dimensional Functionally Graded Plates (2D-FGP) were numerically analyzed for buckling and bending using a finite element model described plate kinematics without a shear correction factor or shear locking treatment.

Coskun et al. [16] by applying general third-order plate theory studied the bending, free vibration, and critical buckling behavior of FG porous microplates. Analytical results were obtained using the Navier method. In the context of third-order plate theory, analyzed the effects of three different porosity distributions on the resulting porosity variations. Kim et al. [17] examined the FG porous microplates for bending, free vibration, as well as buckling responses with classical and first-order shear deformation plate theories. Analysis using Navier's solution of supported rectangular plates was executed. Two material constituents were modeled using power-law distribution across plate thickness. Singh et al. [18] an analytical model for FG thin-walled beam flexural response was developed using first-order shear deformation theory and Vlasov's theory. The power law distribution of mild steel and alumina volume fractions varied material properties along the depth. FG thin beams under uniform vertical loading were numerically analyzed. Mergen et al. [19] established the dynamic and static responses in a nonlinearly forced axially FG tapered beam. Hareram et al. [20], axial FG thin taper beams with different taper profiles and material gradations were studied for free vibration. The mathematical formulation uses energy and that could be resolved in two halves, static as well as dynamic.

Prashik Malhari Ramteke et al. [21] in this study, nonlinear thermal frequency characteristics of multidirectional, double-curved, FG panels are investigated numerically using finite elements. The material properties of the FG panel are estimated utilizing the temperature-dependent individual properties of the FG constituents, Voigt's micromechanical model, and various forms of material distribution patterns. Rajasekarana et al. [22] discussed the mechanical behavior of non-uniform nano-beams. Small-scale effects are described according to the nonlocal strain gradient theory, the beam is represented according to the Euler-Bernoulli beam theory, and non-uniformity with a general change in cross section is postulated. Nguyen et al. [23] beams that are either transversely or axially tapered in FG are analyzed statically. The numerical results show that a T-FG beam behaves differently than an isotropic beam. On the contrary, an A-FG beam behaves exactly like an isotropic beam in terms of axial displacement and stress. Ketabdari et al. [24] using their elastic basis, Winkler and Pasternak analyzed the free vibration in homogenous and FG plates. The elastic foundation was an electric support by Pasternak and Winkler, whose stiffness coefficients varied both parabolically and linearly in each direction. Khoram et al. [25] there were tests conducted on the magnetic and mechanical deflection of FG nanobeams. The

assumption was made that the nanobeam would be supported by the Winkler-Pasternak basis. The mechanical behavior of nanobeams was described by the Timoshenko beam model and the nonlocal elasticity theory of Eringen.

Ammar Melaibari et al. [26] present the first mathematical definition of the dynamical behavior of Bi-Directional Functionally Graded Porous Plates (BDFGPP) resting on a Winkler–Pasternak foundation based on unified higher-order plate theories. Using the kinematic displacement fields, the null shear strain/stress at the bottom and top surfaces of the plate is satisfied without the requirement for a shear factor correction. Mohammadi et al. [27] FG was used to create a core for a composite nanoplate with lipid face sheets to study nonlinear vibrations. There are three distinct types of FG core materials. The viscoelasticity of lipid membranes was studied using the Kelvin-Voigt model. Adapting the Von-Karman hypotheses, a nonlinear differential equation was derived for analyzing vibration in composite nanoplates. Mohammadi et al. [28] used FG material with a lipid core and two layers for vibration analysis. Nonlocal elasticity theory yields nonlinear differential governing equations. Kelvin-Voigt equation modeling lipid layer viscoelasticity. Nejad et al. [29] The phenomenon of buckling in a nanoplate constructed from a BDFG material of arbitrary composition was investigated. Eringen studied micro buckling loads with his nonlocal theory. Using minimum potential energy, the governing equations were derived. Trung-Kien Nguyen et al. [30] new HSDT was proposed for buckling, and free vibration analysis of isotropic and FG sandwich beams. The transverse shear stress distribution was hyperbolic and boundary conditions were satisfied.

Rahmani et al. [31] Timoshenko's beam theory examined FG material size dependence. FG nanobeam material properties varied power law-like along the thickness. Ammar Melaibari et al. [32] offer a novel mathematical framework to represent the static deflection of a Bi-Directionally Functionally Graded (BDFG) porous plate lying on an elastic base. Detailing the validity of the static response produced by middle surface versus neutral surface formulations and the location of the boundary conditions. Şimşek [33] the effects of a shifting load on a Timoshenko beam which is actually made of bi-directional FGM were investigated. Both the width and length of the beam expanded and contracted at an exponential rate. Slimane et al. [34] using HSDT, performed a vibration behavior of a porous, simply supported FG plate. The thickness of the FG porous plate had an effect on the material's behavior.

Ahmad Reshad Noori et al. [35] an effective numerical method for solving the dynamic response of functionally graded porous (FGP) beams is introduced. Along the thickness direction, the elastic modulus and mass density of porous materials are believed to have non-uniform distributions. It is assumed that the standard open-cell metal foam governs the material constitutive law. Thai et al. [36] vibration analysis in an FG beam was determined by HSD theories. Adjustments to the shear strain boundary produce parallel beam surfaces on top and bottom. Vo, et al. [37] FGB static bending and vibration were examined using an enhanced shear deformation theory. Simsek [38] investigated the behavior of the Timoshenko beam made of bidirectional FGM while it was subjected to a varying load. Both the width and length of the beam expanded and contracted at an exponential rate. Chen et al. [39] Timoshenko's beam theory analyzed porous FG beam buckling and statics. Porous composite materials had different thickness-dependent elasticity modules and mass densities.

A displacement-based unified shear deformation theory was developed by Sayyad et al. [40] for advanced composite plates and beams. Transverse shear deformation affected shape function in this theory. Zenkour et al. [41] temperature and humidity impact FG porous beam bending. Normal and shear strains affect this investigation.

Menasria et al. using revised shear deformation theory, the current work present a dynamic analysis of an FG-sandwich plate sat on an elastic foundation with various types of support. The current analytical model is simplified by reducing the number of unknowns. Without inserting correction factors, the free surfaces of the FG-sandwich plate are guaranteed to have zero shear stresses. The study of Prashik Malhari Ramteke et al. [42] describes the massive geometric deformation-induced deformation and stress analysis of a bidirectional (2D) functionally graded material (FGM) shell panel subjected to changing mechanical loads (static and dynamic). The reactions of graded structures are computed numerically using an in-house finite element model with displacement functions of higher order.

Non-classical Timoshenko beam model [43] is created using a variational formulation based on the modified couple stress theory and Gurtin-Murdoch surface elasticity theory to investigate the mechanics of 2D-FG nonuniform micro/nanobeams. The Hamilton principle is used to simultaneously derive the equations of motion and boundary conditions that account for bending and axial deformations, Poisson's effect, and the physical neutral axis concept.

Nguyen et al. [44] analytical solutions for the static analysis of functionally graded transversely or axially tapered cross-section beams are given. Depending on the power form, the beam's elastic modulus changes continuously in the thickness or axial direction.

Samaniego et al. [45] Using DNNs to tackle boundary value problems has been investigated. Many extremely relevant computational mechanics cases have been solved using DNNs to construct the approximation space, demonstrating that it is possible to approach the solution of extremely relevant BVPs using concepts and methods derived from deep learning.

Hongwei et al. [46] Deep Collocation Method (DCM) for thin plate bending problems is proposed in this work. Deep learning employs computational graphs and backpropagation algorithms, which are utilized in this method. In addition, the planned DCM is based on a feed-forward deep neural network (DNN) and varies from the majority of previous deep learning applications for mechanical challenges.

The majority of the research is concentrated on static, dynamic, and buckling studies of conventional, FG one-dimensional, and two-dimensional beams. As a result of this, we are motivated to apply higher-order theory in this research on cross-section (tapered) in FGM. The author is only vaguely aware of a small handful of studies that have been conducted and presented on the subject of the deflection of two-directional tapered FGBs that are predicated on a third-order shear deformation theory

In this study, a comparison is made between the analytical solutions of beam deflection under evenly distributed loads in 2D-FGTB. It is presumable that the material properties in the beam will vary according to a power law distribution in thickness as well as length directions. Simply supported (SS) and Clamped-clamped (CC) beams are subjected to homogenous load with varying length-to-thickness ratios (L/h) and gradient exponents so that the deflection of each type of beam can be compared. Hamilton's principle and RHSDT are used to generate governing equations of motion.

2. Material Properties of FG Tapered Beam

2D-FGTBs are favored in this study. The composition of a material can vary along the length or thickness axes, as well as simultaneously along the length (x-axis) and thickness (z-axis) axes. Material parameters such as Young's modulus ' E,' Poisson's ratio ' μ,' and mass density (ρ) vary (z-axis). The thicknesses at the left and right ends of the non-uniform beams are h_2 and h_1 ($<h_2$), respectively. At any axial location, the thickness h(x) in the tapered beam is given by $h(x) = h_2 [1 - n(x/L)]$. Where n is the taperness parameter given by $n = [1-h_1/h_2]$. In view of this, the present theory is having following important assumptions.

1. The origin of the Cartesian coordinate system is taken at the neutral surface of the FG beam.
2. The transverse normal stress σ_z is negligible in comparison with in-plane stress σ_x.
3. This theory assumes a constant transverse shear stress and requires a shear correction factor to satisfy the lower and upper beam boundary requirements.

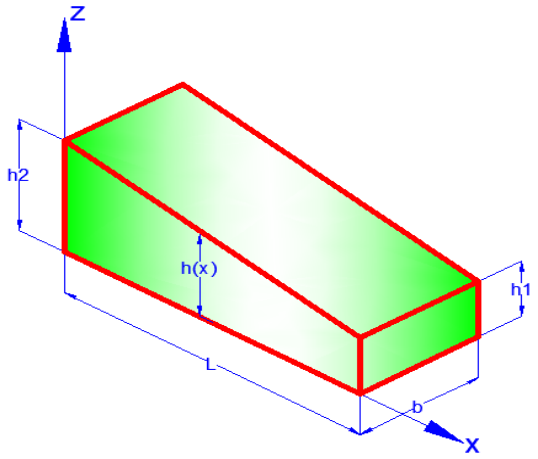

Fig. 1. Geometry of FG Tapered Beam

Due to variations in the volume fraction of constituent materials, the FG beam's properties vary continuously. Assume a functional relationship between thickness coordinate and material property. The volume fraction of metal (V_m) could be expressed based on power law as [43],

$$V_f(x,z) = \left(\frac{x}{L}\right)^{px}\left(\frac{1}{2}+\frac{z}{h(x)}\right)^{pz} \quad (1)$$

Material properties of TDFG tapered beam can be defined as [43]:

$$P(x,z) = (P_c - P_m)\left(\frac{x}{L}\right)^{px}\left(\frac{z}{h(x)}+\frac{1}{2}\right)^{qz} + P_m \quad (2)$$

Metal phases are denoted by "m" and ceramic phases by "c". 'P_x' and 'P_z' stands for power law exponents that indicate the material variation profile through the axial and transverse directions of the beam. The power law exponents are ($p_x = p_z = 0, 0.1, 0.2, 0.3, 0.4, 0.5, 0.6, 0.7, 0.8, 0.9, 1$) as shown in Figure 2.

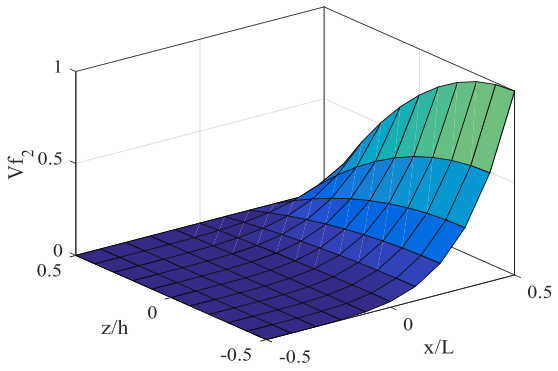

Fig. 2. Assessing metal volume fractions in the z/h and x/L directions.

2.1. 2D-FGTB Formula

Modulus of elasticity "E" Poisson's ratio "μ" and density "ρ" of FG tapered beam are listed below [43].

$$E(x,z) = (E_c - E_m)\left(\frac{z}{h(x)} + \frac{1}{2}\right)^{pz}\left(\frac{x}{L}\right)^{px} + E_m \quad (3)$$

$$\rho(x,z) = (\rho_c - \rho_m)\left(\frac{z}{h(x)} + \frac{1}{2}\right)^{pz}\left(\frac{x}{L}\right)^{px} + \rho_m \quad (4)$$

2.2. Field of displacement and constitutive equations

For the purpose of presenting the displacement equations, Reddy's HSDT with a shear strain function is taken into account [30].

$$u(x,z,t) = u_0(x,t) - z\frac{\partial w_0}{\partial x}(x,t) + f(z)h(x,t) \quad (5)$$

$$w(x,z,t) = w_0(x,t) \quad (6)$$

The axial displacement, transverse displacement shear slope at a given point on the neutral axis is represented by u_0, w_0, $\frac{\partial w_0}{\partial x}$ Determining transverse shear deformation distribution using the inverse elastoplastic function (shape function) i.e. f (z).

$$\varepsilon_x = \frac{\partial U}{\partial x} = \frac{\partial u_0}{\partial x} - z\frac{\partial^2 w_0}{\partial x^2} + f(z)\left(\frac{\partial \phi}{\partial x}\right) \quad (7)$$

$$\varepsilon_z = \frac{\partial w}{\partial z} = 0 \quad (8)$$

$$\gamma_{xz} = \frac{\partial u}{\partial z} + \frac{\partial w}{\partial x} = -\frac{\partial w_0}{\partial x} + f'(z)\emptyset + \frac{\partial w_0}{\partial x} \quad (9)$$

$$\gamma_{xz} = f'(z)\emptyset \quad (10)$$

$$f(z) = z\left[1 - \frac{4}{3}\left(\frac{z}{h}\right)^2\right] \quad (11)$$

$$f'^{(z)} = \left[1 - 4\left(\frac{z}{h}\right)^2\right] \quad (12)$$

where

ε_x = strain in x direction

ε_z = strain in the z − direction

γ_{xz} = shear strain

The beam in functionally graded materials obeys Hooke's law, so the behavioral relations can be given as follows:

$$\begin{Bmatrix}\sigma_x \\ \tau_{xz}\end{Bmatrix} = \begin{bmatrix}Q_{11}(z) & 0 \\ 0 & Q_{55}(z)\end{bmatrix}\begin{Bmatrix}\varepsilon_x \\ \gamma_{xz}\end{Bmatrix} \quad (12a)$$

$$Q_{11}(z) = \frac{E(x,z)}{1-\mu^2} \quad (13)$$

$$Q_{55}(z) = \frac{E(x,z)}{2(1+\mu)} \quad (14)$$

2.3. Laws of Motion Equations

Governing equations derived from the principle of virtual displacements yields, [30].

$$\int_0^T \delta(U+V-K)\,dt=0 \quad (15)$$

where δU is variation strain energy, δk is variation in kinetic energy, δV is variation in work done and t is the time.

$$\delta U = \int_0^L \int_{-\frac{h}{2}}^{\frac{h}{2}} (\sigma_x \delta\varepsilon_x + \tau_{xz}\delta\gamma_{xz})dzdx \quad (16)$$

$$\delta V = -\int_0^L q\delta w_0\,dx \quad (17)$$

The bending stress of the tapered beam in terms of virtual strain energy and work done can be shown by:

$$B = \delta U + \delta V = 0 \quad (18)$$

$$\delta U = \int_0^L \int_{-\frac{h}{2}}^{\frac{h}{2}} (\sigma_x \delta\varepsilon_x + \tau_{xz}\delta\gamma_{xz})dzdx - \int_0^L q\delta w_0\,dx = 0 \quad (19)$$

$$= \int_0^L \int_{-\frac{h}{2}}^{\frac{h}{2}} \left(\sigma_x \delta\left(\frac{\partial u_0}{\partial x} - z\frac{\partial^2 w_0}{\partial x^2} + f(z)\left(\frac{\partial \phi}{\partial x}\right)\right) + \tau_{xz}\delta f'(z)(\emptyset)\right)$$

$$-\int_0^L q\delta w_0 dx = 0 \quad (20)$$

$$= \int_0^L \left(N_x \frac{\partial \delta u_0}{\partial x} - M_b \frac{\partial^2 \delta w_0}{\partial x^2} + M_s \frac{\partial \delta \emptyset}{\partial x} + Q_{xz} \delta \emptyset \right) dx$$

$$- \int_0^L q \delta w_0 dx = 0 \tag{21}$$

$$(N_x,\ M_b,\ M_s) = \int_{-\frac{h}{2}}^{\frac{h}{2}} (1, z, f(z)) \sigma_x \, dz \tag{22}$$

$$\begin{bmatrix} N_x \\ M_b \\ M_s \end{bmatrix} = \int_{-h/2}^{h/2} \sigma_x \begin{bmatrix} 1 \\ z \\ f(z) \end{bmatrix} dz$$

$$= \begin{bmatrix} A_{11} \frac{du_0}{dx} & B_{11} \frac{d^2 w_0}{dx^2} & B^s{}_{11} \frac{d\emptyset}{dx} \\ B_{11} \frac{du_0}{dx} & D_{11} \frac{d^2 w_0}{dx^2} & D^s{}_{11} \frac{d\emptyset}{dx} \\ B^s{}_{11} \frac{du_0}{dx} & D^s{}_{11} \frac{d^2 w_0}{dx^2} & H^s{}_{11} \frac{d\emptyset}{dx} \end{bmatrix} \tag{22a}$$

$$Q_{xz} = \int_{-\frac{h}{2}}^{\frac{h}{2}} \tau_{xz} f'(z) dz \tag{23}$$

where, N_x is axial resultant force, M_b is the resultant bending moment, M_s is resultant moment owing to shear deformation and Q_{xz} are resultant shear forces. By integrating displacement gradations, governing equations of equilibrium can be derived.

$$\delta U_0 : \frac{\partial}{\partial x} N_x = 0 \tag{24}$$

$$\delta w_0 : \frac{\partial^2}{\partial x^2} M_b + q = 0 \tag{25}$$

$$\delta \emptyset : \frac{\partial}{\partial x} M_s + Q_{xz} = 0 \tag{26}$$

$$A_{11} = \int_{-h/2}^{h/2} Q_{11}(z)\, dz \tag{27}$$

$$B_{11} = \int_{-h/2}^{h/2} Q_{11}(z)\, z dz \tag{28}$$

$$D_{11} = \int_{-h/2}^{h/2} Q_{11}(z)\ z^2 dz \tag{29}$$

$$B^s{}_{11} = \int_{-h/2}^{h/2} Q_{11}(z) f(z)\, dz \tag{30}$$

$$D^s{}_{11} = \int_{-h/2}^{h/2} Q_{11}(z) z f(z) dz \tag{31}$$

$$H^s{}_{11} = \int_{-h/2}^{h/2} Q_{11}(z) [f(Z)]^2 dz \tag{32}$$

The motion equations admit Navier's solutions applied to get analytical results for the various boundary conditions. The coefficients $u_0, w_0 \, and \, \emptyset$ can be written assuming the following variations:

$$\begin{bmatrix} u_0 \\ w_0 \\ \emptyset \end{bmatrix} = \sum_{m=1,3,5}^{\infty} \begin{bmatrix} u_m \cos\alpha\, x e^{i\omega t} \\ w_m \sin\alpha\, x e^{i\omega t} \\ \emptyset_m \cos\alpha\, x e^{i\omega t} \end{bmatrix} \tag{33}$$

where u_0, w_0 and ϕ are unknown coefficients, and complex number $i = \sqrt{-1}$ and $\alpha = m\pi/L$.

The transverse load q is also expressed by double series of Fourier sine as follows:

$$q = \sum_{m=1,3,5}^{\infty} \frac{4q_0}{m\pi} \sin\alpha x \tag{34}$$

Substitute the expressions $u_0, w_0 \, and \, \emptyset$ of Eq. (33) in the equations of motion (24), (25), and (26). The analytical solutions are given in the following form:

$$\begin{bmatrix} s_{11} & s_{12} & s_{13} \\ s_{12} & s_{22} & s_{23} \\ s_{13} & s_{23} & s_{33} \end{bmatrix} \begin{Bmatrix} u_m \\ w_m \\ \emptyset_m \end{Bmatrix} = \begin{Bmatrix} 0 \\ \frac{4q_0}{m\pi} \\ 0 \end{Bmatrix} \tag{35}$$

$$S_{11} = \int_{-h/2}^{h/2} Q_{11}(z)\, dz\, (m\pi/L)^2 \tag{36}$$

$$S_{12} = -\int_{-h/2}^{h/2} Q_{11}(z)\, z dz\, (m\pi/L)^3 \tag{37}$$

$$S_{13} = \int_{-h/2}^{h/2} Q_{11}(z) z f(z)\, dz\, (m\pi/L)^2 \tag{38}$$

$$S_{22} = \int_{-h/2}^{h/2} Q_{11}(z) f(z)\, dz\, (m\pi/L)^2 \tag{39}$$

$$S_{23} = -\int_{-h/2}^{h/2} Q_{11}(z) z f(z)\, dz\, (m\pi/L)^2 \tag{40}$$

$$S_{33} = \int_{-h/2}^{h/2} Q_{11}(z) [f(z)]^2 dz\, (m\pi/L)^2 \tag{41}$$

3. Results and Discussion

To foretell the static analysis of the 2D-FGTB subject to several boundary conditions, such as for SS and CC, the HSDT-based numerical studies presented in Table 1 are carried out.

Deflection analysis is presented and validates the accuracy of the current theory. 2D-FGTB is considered for numerical results made of Alumina and Aluminum with material properties as follows.

Alumina: E_c=380 Gpa, $\rho_c = 3960 \frac{\text{kg}}{\text{m}^3}$, μ_c = 0.3

Aluminum: E_m=70 Gpa, $\rho_m = 2702 \frac{\text{kg}}{\text{m}^3}$, μ_m = 0.3

Table 1. Kinematic boundary conditions can be applied to numerical calculations.

Boundary condition	X= -L/2	X= L/2
Simply Supported	u=0, w=0	w=0
Clamped-Camped	u=0, w=0, ϕ=0, w'=0	u=0,w=0, ϕ=0, w'=0

Transverse deflection ($\overline{w}$)

$$\overline{w} = \frac{w100E_m h(x)^3}{q_0 L^4} \tag{42}$$

$\overline{w}$ = transverse deflection

w = transverse deflection at any point in the beam

E_m = Young's modulus of the metal

$h(x)$ = Height of taper beam

q_0 = load

L = Length of beam

3.1. Validation

A methodical and exhaustive validation of the 2D-FGTB with higher-order shear deformation theory was conducted. Eq. (42) represents the nondimensional deflection. The results presented in Table 2 are based on idealized beams with different boundary conditions. The results from the current code differ marginally from those reported by Rabab et al. [43]. The deflection results of Table 3 are also identical for the CC beam.

Table 2. Comparison of dimensionless transverse deflection ($\overline{w}$) values of SS 2D-FGTB with different aspect ratios (L/h=5, 20), taper ratio (n=0.1), and gradation exponents(p).

Theory	P=0	P=0.5	P=1	P=2	P=5	P=10
			L/h=5			
TBT [43]	1.1306	0.6536	0.5671	0.5133	0.4831	0.4777
HSDT	1.0714	0.6466	0.5541	0.5025	0.4495	0.4180
% Error	5.23%	1.07%	2.29%	2.1%	6.9%	12.4%
--			L/h=20			
HSDT	1.0562	0.6057	0.5114	0.4657	0.4126	0.3663

Table 3. Comparison of dimensionless transverse deflection ($\overline{w}$) values of CC 2D-FGTB with different aspect ratios (L/h=5, 20), taper ratio (n=0.1), and gradation exponents(p).

Theory	P=0	P=0.5	P=1	P=2	P=5	P=10
			L/h=5			
HSDT	0.2143	0.1268	0.1131	0.1013	0.0862	0.0836
			L/h=20			
HSDT	0.2071	0.1151	0.1003	0.0862	0.0750	0.0643

Table 4. Dimensionless transverse deflection ($\overline{w}$) values of 2D-FGTB with different aspect ratio (L/h=5, 20), taper ratio (n=0.1), and gradation exponents (p_x, p_z).

n	pz	Px					
		0	0.5	1	2	5	10
				L/h=5			
0.1	0	0.2143	0.1402	0.1341	0.1233	0.1093	0.0986
	0.5	0.2115	0.1268	0.1236	0.1144	0.1034	0.0976
	1	0.2087	0.1265	0.1131	0.1156	0.0974	0.0902
	2	0.2059	0.1206	0.1046	0.1013	0.0915	0.0888
	5	0.2031	0.1148	0.0999	0.0920	0.0862	0.0846
	10	0.2004	0.1104	0.0926	0.0879	0.085	0.0836
				L/h=20			
0.1	0	0.2071	0.1384	0.1185	0.1089	0.0946	0.0812
	0.5	0.2043	0.1325	0.1094	0.1014	0.0897	0.0771
	1	0.2016	0.1265	0.1003	0.0938	0.0848	0.0711
	2	0.1988	0.1206	0.0911	0.0862	0.0799	0.0674
	5	0.1960	0.1147	0.0888	0.0787	0.0750	0.0658
	10	0.1932	0.1087	0.0847	0.0742	0.0701	0.0643

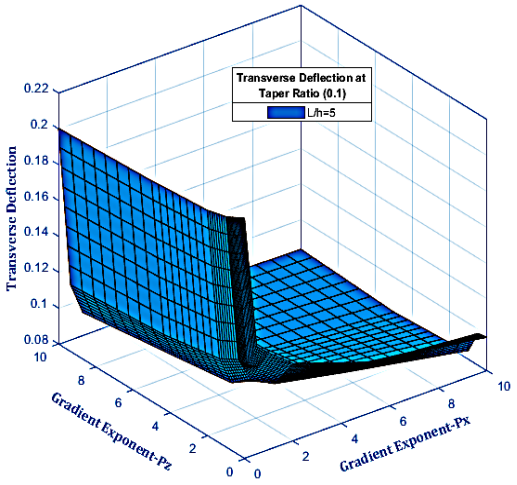

Fig. 3. Dimensionless transverse deflection ($\overline{w}$) values of CC TDFG tapered beam at aspect ratios (L/h=5), taper ratio (n=0.1).

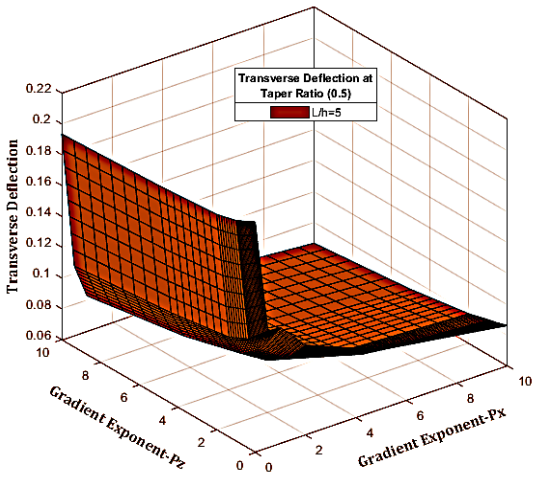

Fig. 4. Dimensionless transverse deflection ($\overline{w}$) values of CC 2D-FGTB at aspect ratios (L/h=5), taper ratio (n=0.5).

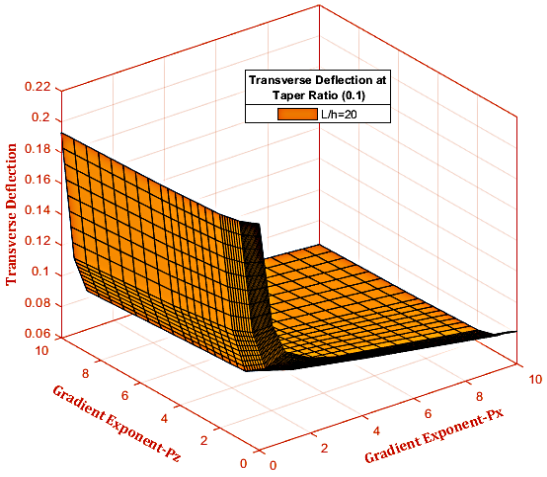

Fig. 5. Dimensionless transverse deflection ($\overline{w}$) values of CC TDFG tapered beam at aspect ratios (L/h=20), taper ratio (n=0.1).

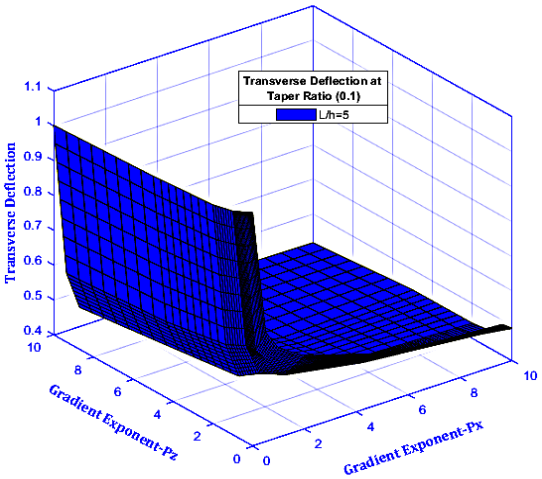

Fig. 7. Dimensionless transverse deflection ($\overline{w}$) values of SS 2D-FGTB at aspect ratios (L/h=5), taper ratio (n=0.1).

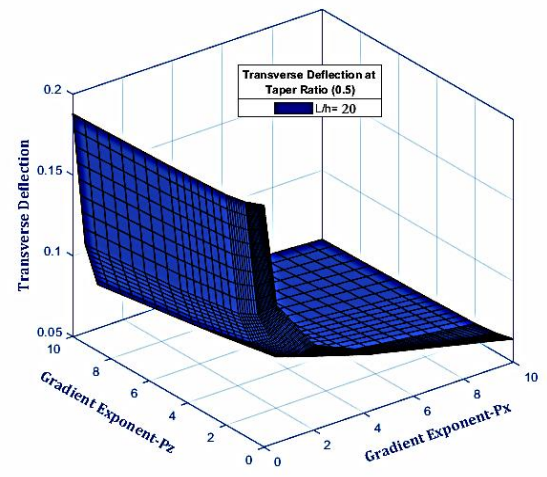

Fig. 6. Dimensionless transverse deflection ($\overline{w}$) values of CC 2D-FGTB at aspect ratios (L/h=20), taper ratio (n=0.5).

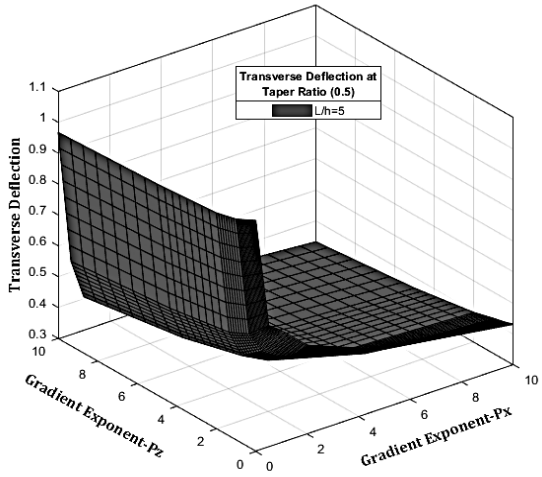

Fig. 8. Dimensionless transverse deflection ($\overline{w}$) values of SS 2D-FGTB at aspect ratios (L/h=5), taper ratio (n=0.5).

Table 5. Dimensionless transverse deflection ($\overline{w}$) values of SS 2D-FGTB with different aspect ratio (L/h=5, 20), taper ratio (n=0.5).

n	pz	px					
		0	0.5	1	2	5	10
		L/h=5					
0.1	0	1.0714	0.7151	0.6570	0.6114	0.5443	0.4928
	0.5	1.0575	0.6466	0.6055	0.5675	0.5147	0.4882
	1	1.0436	0.6452	0.5541	0.5236	0.4851	0.4512
	2	1.0296	0.6152	0.5125	0.5025	0.4654	0.4435
	5	1.0157	0.5853	0.4896	0.4565	0.4495	0.4229
	10	1.0018	0.5631	0.4537	0.4362	0.4237	0.4180
		L/h=20					
0.1	0	1.0562	0.6850	0.6046	0.5883	0.5205	0.4628
	0.5	1.0421	0.6557	0.5580 0.5114	0.5474	0.4935	0.4396
	1	1.0279	0.6263	0.5114	0.5066	0.4665	0.4054
	2	1.0137	0.5969	0.4648	0.4657	0.4396	0.3839
	5	0.9996	0.5676	0.4527	0.4249	0.4126	0.3751
	10	0.9854	0.5382	0.4321	0.4009	0.3857	0.3663

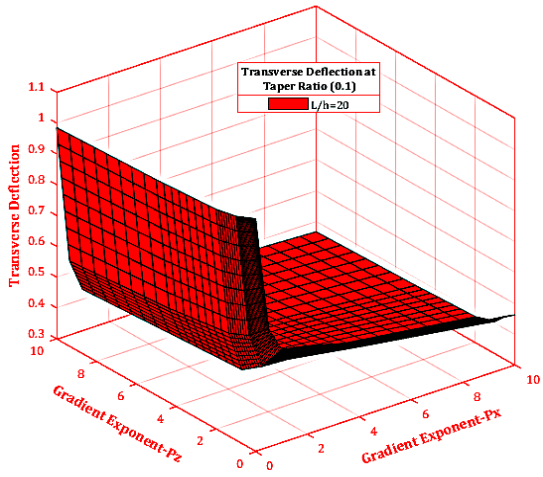

Fig. 9. Dimensionless transverse deflection ($\overline{w}$) values of SS 2D-FGTB at aspect ratios (L/h= 20), taper ratio (n=0.1).

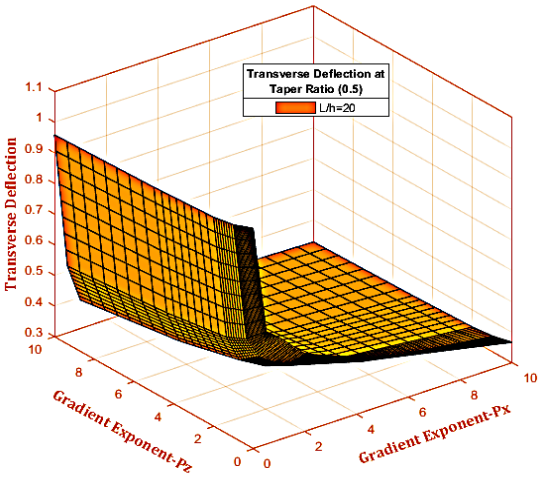

Fig. 10. Dimensionless transverse deflection ($\overline{w}$) values of SS 2D-FGTB at aspect ratios (L/h= 20), taper ratio (n=0.5).

The results of transverse deflections of the present theory are compared with the results of a taper nano beam [43] for SS boundary conditions. It is found that the results are agreeable. The remaining values are also acceptable for CC as well.

The effects of non-uniform parameters on thickness variation, *h(x),* and on the maximum dimensionless deflection at different power-law exponents and supporting types are presented ahead.

In this scenario, the width of the beam is constant; therefore, the applied distribution load is constant along the beam, but the moment of inertia and elastic modulus change along the length of the beam. The variation of the moment of inertia is due to the thickness variation along the length of the beam. It is obvious that, for all supported types, the maximum dimensionless deflection decreases as shown in Tables 4, and 5.

while the non-uniformity parameter decreases 'n' and the rate of increase depends on the supporting types as shown in Figures 3-6 for the CC beam and Figures 7-10 for the SS beam.

The maximum rate of dimensionless deflection appears in the SS beam as shown in Table 5, in comparison with other supports like CC as shown in Table 4. The main factors that affected the maximum dimensionless deflection and its rate of change are the distribution of the young modulus, the position of the clamped end, and the change in moment of inertia.

Generally, the width variation effects are not significant on the deflection in the beam in comparison with the thickness variation effects and the combination of both width and thickness variations, where it has the greater effects. In other words, the effects of variations mean that the dimensionless deflection increases as the non-uniformity parameters are reduced. For SS beam the effects of width variation, thickness variation, and both width and thickness variation cause to increase in the dimensionless deflection, in addition to changing the position of maximum dimensionless deflection. Generally, the mid-span is the position of the maximum deflection in a SS beam (i.e., x = l/2). It seems that the position of dimensionless deflection is changed due to the variation in the dimensions of the beam and the distribution of elastic modulus.

The effects of aspect ratio (L/h) on the maximum dimensionless deflection, when the aspect ratio increases the maximum dimensionless deflection decrease as shown in Figure 5, Figure 6 as compared with Figure 3, Figure 4 for CC beam, and Figure 9, Figure 10 as compared with Figure 7, Figure 8 for SS beam due to the structure becomes relatively narrower or shorter in one direction compared to the other, which reduces its bending stiffness and makes it more susceptible to deflection under load.

4. Conclusions

Using a variational formulation based on Reddy's higher-order shear deformation theory, a new 2D-FGTB model is developed in this article. In order to derive the equation of motion and corresponding boundary conditions that account for deflection and the neutral axis concept, the Hamilton principle is utilized simultaneously. In addition to the material properties, the model includes a material length scale parameter and surface elasticity constants that vary along the axial and transverse directions of the beam according to a power law.

Navier's method is applied to develop a 2D-FGTB model to derive an analytical solution for the deflection responses of simply supported and clamped-clamped 2D-FGTB. A comprehensive parametric study is performed to investigate the effect of various material and geometrical parameters on the deflection responses. The principal findings can be summed up as follows:

1. The structure effect and surface residual stress increase the beam's stiffness, thereby decreasing the predicted deflection.
2. Increasing the gradient exponents in the beam's thickness pz and/or length px increases the beam's stiffness-hardening, thereby reducing its static deflection.
3. The stiffness-hardening effect of the taper beam decreases its static deflection proportionally to the aspect ratio of the material.
4. The influence of the taperness parameters is reduced when the structure and surface effects are incorporated.

Boundary conditions: Reddy's HSDT assumes that the plate's edges are simply supported or clamped. However, in practice, plates may have more complex boundary conditions, such as free or partially clamped edges, which can affect the analysis accuracy.

References

[1] Armagan Karamanli, 2018. Analytical Solutions for Buckling Behavior of Two Directional FG Beams Using a Third Order Shear Deformable Beam Theory. Academic Platform Journal of Engineering and Science, 6(2), pp. 164-178.

[2] Parham Zahedinejad, Chen Zhanga, Haifeng Zhanga, Ju Shuai, 2020. A comprehensive review on vibration analysis of functionally graded beams. International Journal of Structural Stability and Dynamics, Doi: 10.1142/S0219455420300025.

[3] Shahrjerdi A, Mustapha F, Bayat M. and Majid D.L.A., 2011. Free Vibration Analysis of Solar FG Plates with Temperature Dependent Material Properties Using Second Order Shear Deformation Theory. Journal of Mechanical Science and Technology, 25(9), pp. 2195-2209.

[4] Krzysztof Magnucki and Jerzy Lewinski., 2019. Bending of Beams with Symmetrically Varying Mechanical Properties under Generalized Load – Shear effect. Engineering Transactions, 67(3), pp. 441–457.

[5] Pankaj, K., Chauhan and Khan, I.A., 2014. Review on Analysis of FG Material Beam Type Structure. International Journal of Advanced Mechanical Engineering, 4(3), pp. 299-306.

[6] Zidi, A, Tounsi, M.S., Houari, A. and Bég, O.A., 2014. Bending Analysis of FGM Plates UnderHygro-Thermo-Mechanical Loading Using a Four Variable Refined Plate Theory. Aerospace Science Technology, 34, pp. 24–34.

[7] Bouremana M, Houari M.S.A., Tounsi, A., Kaci, A. and AddaBedia E.A., 2013. A New First Shear Deformation Beam Theory Based on Neutral Surface Position for FGB. Steel Composite Structures, 15(5), pp. 467-479.

[8] FoudaNoha, Tawfik El-midany and Sadoun AM., 2017. Bending, Buckling and Vibration of a FG Porous Beam Using Finite Elements. Journal of applied and computational mechanics, 3, pp. 274-282.

[9] Bouremana M, Houari M.S.A., Tounsi, A., Kaci, A. and Adda Bedia E.A., 2013. A New First Shear Deformation Beam Theory Based on Neutral Surface Position for FGB. Steel Composite Structures, 15(5), pp. 467-479.

[10] Bouafia, K., Kaci, A., Houari, M.S.A., Benzair, A. and Tounsi, A., 2017. A Nonlocal Quasi-3D Theory for Bending and Free Flexural Vibration Behaviors of FGNanobeams. Smart Structures and Systems, 19(2), pp. 115-126.

[11] Ebrahimi and Barati. 2016. A nonlocal higher-order shear deformation beam theory for vibration analysis of size dependent FGnanobeams. Arabian Journal for Science and Engineering, 41(5), pp. 1679-1690.

[12] Dragan Cukanovi, AleksandarRadakovi, GordanaBogdanovi, MilivojeMilanovi, HalitRedžovi and Danilo Dragovi., 2018. New Shape Function for the Bending Analysis of FG Plate. Materials, 11.

[13] Sayyad, A.S. and Ghugal, Y.M., 2017. A Unified Shear Deformation Theory for the Bending of Isotropic, FG, Laminated and Sandwich Beams and Plates. International Journal of Applied Mechanics, 9(1), pp. 1–36.

[14] Prashik, M. R., Vikash, K., Nitin, S. and Subrata, K.P., 2022. Geometrical nonlinear numerical frequency prediction of porous functionally graded shell panel under thermal environment. International Journal of Non-Linear Mechanics, 143.

[15] Thom Van Do, DinhKien Nguyen, Nguyen DinhDuc, Duc Hong Doan and Tinh Quoc Bui., 2017. Analysis of Bi-Directional FG Plates by FEM and a New Third-Order Shear Deformation Plate Theory. Thin Walled Structures, 119, pp. 687-699.

[16] Semsi Coskun, Jinseok Kim and HoussamToutanji., 2019. Bending, Free Vibration, And Buckling Analysis of FG Porous Micro-Plates Using a General Third-Order Plate Theory. J. Compos. Sci., 3(15).

[17] Jinseok Kim, Krzysztof KamilZur and Reddy, J.N., 2018. Bending, Free Vibration, and Buckling of Modified Couples Stress-Based FG Porous Micro-Plates. Composite Structures.

[18] Singh, S.B., Himanshu Chawla and Aditya Narkhede., 2019. Flexural Analysis of FG thin Walled Beams. Proc Indian Natn Sci. Acad., 85(4), pp. 829-842.

[19] Mergen, H. and Hamed, F., 2017. Bending and vibration analyses of coupled axially FG tapered beams. Nonlinear Dyn.

[20] Hareram, L., Anirban, M. and Sarmila S., 2016. Geometric Nonlinear Free Vibration of Axially FG Non-Uniform Beams Supported on Elastic Foundation. Curved and Layer. Structures, 3(1), pp. 223–239.

[21] Prashik, M.R., Subrata Kumar, P. and Nitin Sharma, 2022. Nonlinear Vibration Analysis of Multidirectional Porous Functionally Graded Panel under Thermal Environment. American Institute of Aeronautics and Astronautics, 60.

[22] Rajasekarana, S. and Hossein, B.K., 2017. Bending, buckling and vibration of small-scale tapered beams. International Journal of Engineering Science, 120, pp. 172–188.
[23] Nguyen, N.T., Kim, N.I., Cho, I., Phung, Q.T. and Lee, J., 2014. Static analysis of transversely or axially FG tapered beams. Materials Research Innovations, 18.
[24] Ketabdari, M.J., Allahverdi, A., Boreyri, S. and Ardestani, M.F., 2016. Free vibration analysis of homogeneous and FGM skew plates resting on variable Winkler-Pasternak elastic foundation; Mechanics & Industry, 17(1).
[25] Khoram, M.M., Hosseni, M.M., Hadi, A. and Shishehsaz, M., 2020. Bending analysis of bidirectional FGM Timoshenko nanobeam subjected to mechanical and magnetic forces and resting on Winkler–Pasternak foundation. International Journal of Applied Mechanics, 12(08), 2050093.
[26] Ammar Melaibari, Salwa A. Mohamed, Amr E. Assie, Rabab A. Shanab and Mohamed A. Eltaher, Free Vibration Characteristics of Bidirectional Graded Porous Plates with Elastic Foundations Using 2D-DQM, Mathematics 2023, 11(1), 46.
[27] Mohammadi, M. and Rastgoo, A., 2019. Nonlinear vibration analysis of the viscoelastic composite nanoplate with three directionally imperfect porous FG core. Structural Engineering and Mechanics an Int'l Journal, 69(2), pp. 131-143.
[28] Mohammadi, M. and Rastgoo A., 2020. Primary and secondary resonance analysis of FG/lipid nanoplate with considering porosity distribution based on a nonlinear elastic medium. Mechanics of Advanced Materials and Structures, 27(20), pp. 1709-1730.
[29] Nejad, M.Z., Maryam, E., Sima, Z. and Hadi, A., 2016. Buckling analysis of arbitrary two-directional FG Euler–Bernoulli nano-beams based on nonlocal elasticity theory. International Journal of Engineering Science, 103, pp. 1-10.
[30] Nguyen, T.K., Nguyan, T.P., Vo, T.P. and Thai, H.T., 2015. Vibration and buckling analysis of functionally graded sandwich beams by a new higher-order shear deformation theory. Composites part-B: Engineering, 76, pp. 273-285.
[31] Rahmani, O. and Pedram, O., 2014. Analysis and modeling the size effect on vibration of FG nanobeams based on nonlocal Timoshenko beam theory. International Journal of Engineering Science, 77, pp. 55-70.
[32] Ammar Melaibari, Salwa A. Mohamed, Amr E. Assie, Rabab A. Shanab, and Mohamed A. Eltaher, Static Response of 2D FG Porous Plates Resting on Elastic Foundation Using Midplane and Neutral Surfaces with Movable Constraints. Mathematics, 10(24), 4784.
[33] Şimşek, M., 2015. Bi-directional functionally graded materials (BDFGMs) for free and forced vibration of Timoshenko beams with various boundary conditions. Composite Structures, 133, pp. 968-978.
[34] Slimane, M., Samir, B., Hakima, B. and HadjMostefa, A., 2019. Free vibration analysis of FG plates with porosities. International Journal of Engineering Research & Technology (IJERT), 8(03), pp. 143-147.
[35] AhmadReshad Noori, Timuçin Alp Aslan, Beytullah Temel, 2021. Dynamic Analysis of Functionally Graded Porous Beams Using Complementary Functions Method in the Laplace Domain. Composite Structures, 256, 113094.
[36] Thai, H.T. and Vo, T.P., 2012. Bending and free vibration of FG beams using various higher-order shear deformation beam theories. International journal of mechanical sciences, 62(1), pp. 57-66.
[37] Vo, T.P., Thai, H.T., Nguyen, T.K. and Inan, F., 2014. Static and vibration analysis of FG beams using refined shear deformation theory. Meccanica, 49(1), pp. 155-168.
[38] Simsek, M., 2015. Bi-Directional functionally graded materials (BDFGMs) for free and forced vibration of Timoshenko beams with various boundary conditions. Compos Struct. 133(1).
[39] Chen, D., Yang, J. and Kitipornchai, S., 2015. Elastic buckling and static bending of shear deformable FG porous beam.compos. Struct, 133.
[40] Sayyad, A.S. and Ghugal, Y.M., 2017. A unified shear deformation theory for the bending of isotropic, FG, laminated and sandwich beams and plates. Int. j appl. Mechanics, 9(1).
[41] Zenkour, A.M. and Radwan, A.F., 2019. Bending response of FG plates resting on elastic foundations in hygro thermal environment with porosities. compos. struct. 213, pp. 133-143.
[42] Prashik Malhari Ramteke, Subrata Kumar Panda, 2023. Nonlinear static and dynamic response prediction of bidirectional doubly-curved porous FG panel and experimental validation. Composites Part A: Applied Science and Manufacturing, 166.
[43] Rabab, A.S and Mahamed, A.A., 2021. On bending, buckling and free vibration analysis of 2D-FG tapered Timoshenko nanobeams based on modified couple stress

and surface energy theories. Waves in Random and Complex Media.

[44] Nguyen, N.T., Kim, N.I., Cho, I., Phung, Q.T and J. Lee, J., 2014. Static analysis of transversely or axially functionally graded tapered beams. Materials Research Innovations, 18.

[45] Samaniegoc, E., Anitescud, C., Goswamid, S., Nguyen-Thanhe, V.M., Guoe, H., Hamdiae, K., Zhuange, X and Rabczuk, T, 2020. An energy approach to the solution of partial differential equations in computational mechanics via machine learning: Concepts, implementation and applications. Computer Methods Applied Mechanics Engineering. 362,112790.

[46] Hongwei Guo, Xiaoying Zhuang and Timon Rabczuk, 2019. A Deep Collocation Method for the Bending Analysis of Kirchhoff Plate. CMC, 59, pp.433-456.